

Correlation Between Electrochemical and Standard Testing of Aluminum Alloys

Matjaž Finšgar, Irena Lesjak, Varužan M. Kevorkijan, and Marko Degiampietro

Abstract

We report on a corrosion study involving different aluminum alloys from series 2xxx (AA2011, AA2014, AA2024, AA2030, and EN AW 2030) in a 5 wt.% NaCl water solution. The corrosion was investigated using the standard PV113 test and a series of different electrochemical measurements (chronopotentiometry, electrochemical impedance spectroscopy, and cyclic polarization) lasting for 72 h. A possible correlation between the maximum penetration depth due to corrosion into the base material, caused by the standard PV113 test, and the time of electrochemical fatigue was investigated. It was found that a linear correlation exists between the penetration depth in the base material and the electrochemical fatigue time for most of the alloys tested. Moreover, a correlation between the electrochemical fatigue methods and the PV113 test exists for the materials that were the most susceptible to intergranular corrosion. We demonstrated that electrochemical fatigue is suitable for inducing intergranular corrosion.

Keywords

Aluminum alloys • Corrosion study • PV 113 test • Electrochemical testing • Penetration depth • Correlation

Introduction

The motivation for this work was the development of an alternative industrial methodology for controlling the corrosion of aluminum alloys based on electrochemical testing

M. Finšgar

Faculty of Chemistry and Chemical Technology, The University of Maribor, Smetanova ulica 17, 2000 Maribor, Slovenia

I. Lesjak · V. M. Kevorkijan (✉) · M. Degiampietro
Impol Aluminium Industry, Partizanska 38, 2310 Slovenska Bistrica, Slovenia

e-mail: varuzan.kevorkijan@impol.si

of the samples in a 5% NaCl solution. For this purpose, the corrosion behaviors of different aluminum alloys from series 2xxx (AA2011, AA2014, AA2024, AA2030, and EN AW 2030) were investigated using the standard PV113 test and a series of different electrochemical measurements (chronopotentiometry, electrochemical impedance spectroscopy, and cyclic polarization) lasting for 72 h. Particular attention was paid to finding a possible correlation between the maximum penetration depth due to corrosion into the base material, caused by the standard PV113 test, and the time of the electrochemical fatigue.

Experimental

The working electrodes (various aluminum alloys from series 2xxx) were first cleaned with pure acetone and then with a solution of 50 vol.% acetone/50 vol.% deionized water in an ultrasonic bath. The working electrodes were then washed with deionized water.

The measurements were performed using a flat sample clamping cell and an o-ring (Autolab electrochemical cell), an Ag/AgCl (saturated KCl) reference electrode, and a stainless-steel auxiliary electrode. The 5% NaCl solution (corrosive medium) had a volume of 130 mL. The electrochemical measurements were performed at room temperature (laboratory conditions 23 ± 2 °C) with an Autolab PGSTAT204 potentiostat/galvanostat (Metrohm Autolab B. V., Utrecht, The Netherlands). The measurements were monitored with Nova 2.0 (Autolab) software.

The measurements of the **electrochemical impedance spectroscopy (EIS)** were performed in the frequency range from 100 kHz to 5 MHz, and an amplitude of 10 mV at **the open-circuit** (also known as **the corrosion**) **potential (E_{oc})**. The measurements were performed after 1, 3, 5, 7, 10, 15, 20, 24, 36, 48, 60, and 72 h of immersing the electrode in the 5% NaCl solution.

Cyclic polarization (CP) measurements were performed after 72 h of immersion. The measurements were performed in the anodic direction of the potential scan in the potential range of -0.250 V versus E_{oc} to the switching potential at which the current reached 1 mA. After the switching potential, the measurement was performed in the cathodic direction up to the initial potential. The potential scan rate was 0.1 mV/s.

Electrochemical fatigue to induce intergranular corrosion was performed at different time intervals. Because the CP curves in the forward scan did not form typical breakdown potentials and show the shape of the active corrosion curves, a potential that was 20 mV more positive than E_{oc} (as recommended by the ASTM and ISO standards) was used for the fatigue. After the electrochemical fatigue, the samples were analyzed using metallographic tests.

The microstructural investigations were performed after each re-metallographic preparation of the samples, with each sample being metallographically prepared four times. Microstructural images with a maximum depth of the etching after a cross section of the sample were measured in most cases at $500 \times$ magnification.

Results and Discussion

E_{oc} Measurements as a Function of Immersion Time

The chronopotentiometric measurements were performed from the beginning of the immersion until the subsequent EIS measurement. An EIS measurement was then performed, followed by another chronopotentiometric

measurement. This process continued until the measurements of the CP curve. The measurements were performed at least three times (one of the measurements for each alloy is shown in Fig. 1). Between the curves showing the color change in Fig. 1, an EIS measurement was performed. The chronopotentiometric measurements provided us with information about achieving the steady state, which is essential prior to the EIS measurements. In this way, we also obtain information about the destructiveness/non-destructiveness of the EIS measurements. Destructiveness would be indicated if the start of the chronopotentiometric measurement was at a significantly different E_{oc} than the E_{oc} measured at the end of the previous chronopotentiometric measurement. Figure 1 shows that this did not happen, which means that EIS is a non-destructive technique. Since the E_{oc} did not change significantly during a few hours of exposure, it can be concluded that the steady state was achieved, which is a requirement for the EIS measurements.

Electrochemical Impedance Spectroscopy Measurements

EIS is probably the most important electrochemical technique for studying corrosion. It was used to monitor the time dependence of the corrosion for five different aluminum alloys from series 2xxx. The EIS measurements were performed during 1, 3, 5, 7, 10, 15, 20, 24, 36, 48, 60, and 72 h of immersion in a 5% NaCl solution. All the measurements were repeated at least three times.

Based on the collected data, the Nyquist spectra, the impedance Body spectra, and the phase-angle impedance

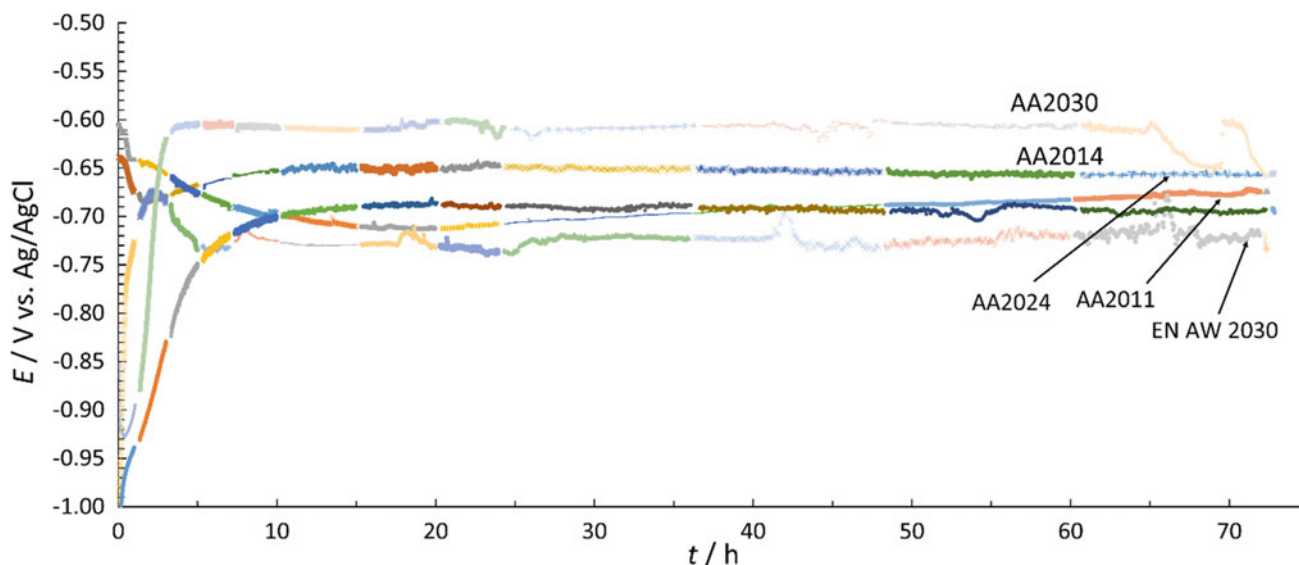


Fig. 1 E_{oc} change for alloys AA2024, EN AW 2030, AA2014, AA2011, and AA2030 as a function of exposure time in 5% NaCl solution

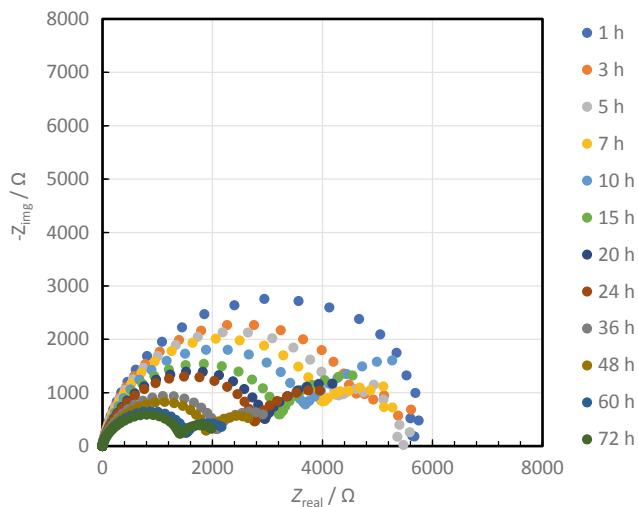


Fig. 2 EIS measurements of the alloy AA2024: Nyquist spectra

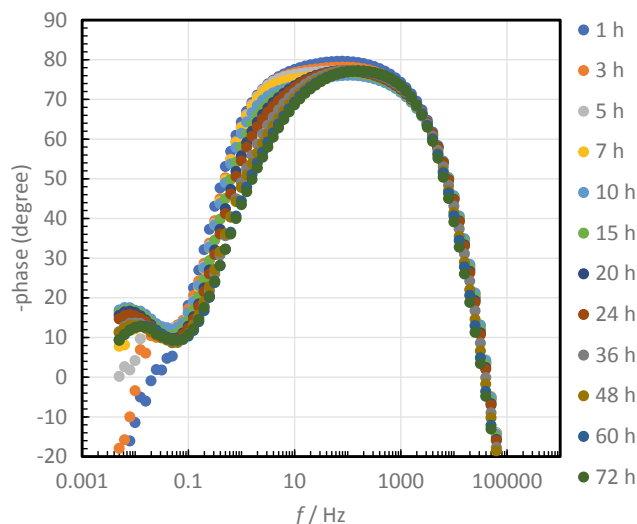


Fig. 4 EIS measurement of the alloy AA2024: Phase-angle impedance spectra

spectra were plotted for each of the five alloys from series 2xxx. As an example, the spectra obtained for the alloy AA2024 are reported in Figs. 2, 3 and 4.

The Nyquist spectra (Fig. 2) represent the negative of the imaginary ($-Z_{imag}$) versus the real part (Z_{real}) of the complex impedance of individual electrodes or electrochemical cells. The impedance Bode spectra (Fig. 3) consists of two plots in one. The x-axis is a logarithmic scale of the frequency (f) and the y-axis is the logarithm of the impedance (Z). Finally, the phase-angle impedance spectra (Fig. 4) represents the symmetry of the phase-angle response with the logarithm of the frequency (f).

General (also known as uniform) corrosion is a phenomenon where a metallic material corrodes evenly over the

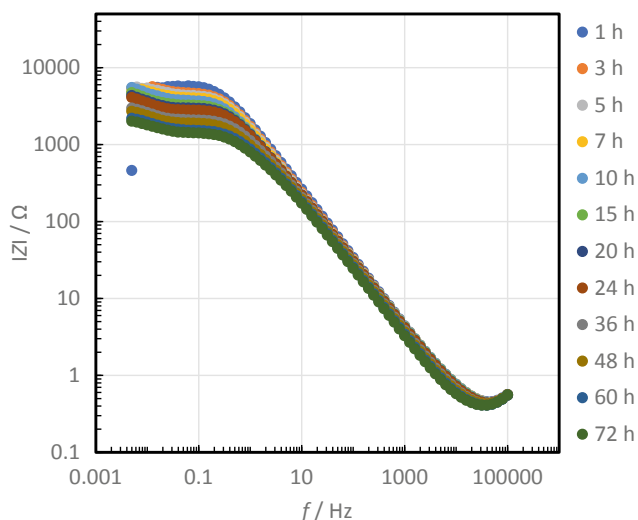


Fig. 3 EIS measurement of the alloy AA2024: Impedance Bode spectra

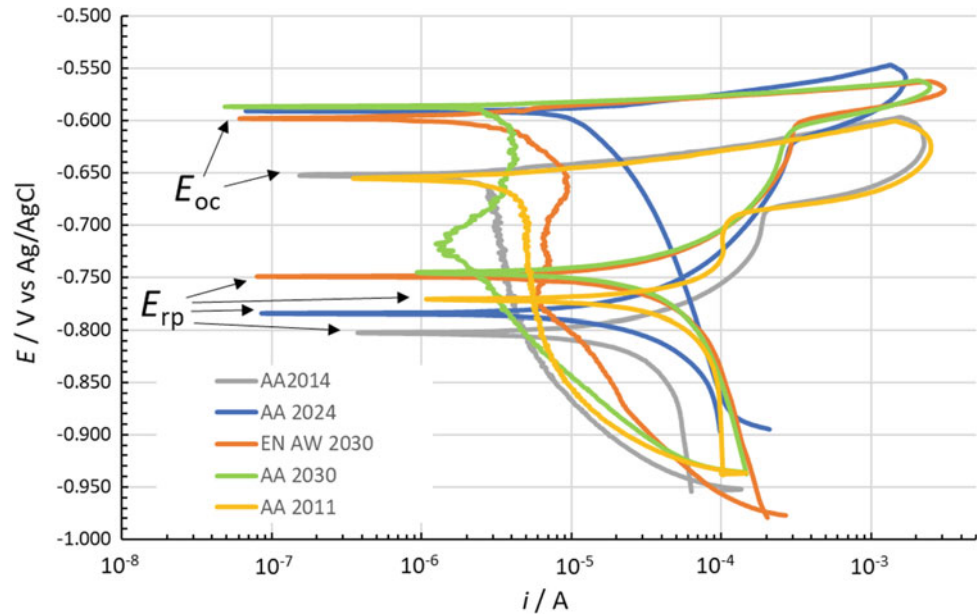
entire surface. The general corrosion rate of the AA2024 and AA2030 alloys increases for up to 72 h of exposure. In the case of the AA2024 alloy, the change in the general corrosion rate with the exposure time is higher than in the case of the AA2030 alloy. The general corrosion rate for the AA2011 alloy increases for 48 h and then stabilizes. The general corrosion rate of the EN AW 2030 alloy is constant in the time interval from 1 to 72 h. The general corrosion rate of the AA2014 alloy is the slowest after 5 h of exposure, after which it increases slightly.

The value of the polarization resistance (R_p) provides us with a measure of how the alloy resists general corrosion. The higher the value of R_p , the more corrosion resistant is the alloy. To determine the corrosion rate, we used a measurement after 72 h of exposure (this exposure time is long enough for the corrosion rate to stabilize and become representative of the alloy). The resistance to general corrosion follows the trend AA2014 > AA2011 > AA2030 > EN AW 2030 > AA2024 (the values are shown in Table 1). The same trend is shown by the Tafel curves (from which it is possible to estimate the corrosion current: the lower the corrosion current, the slower the corrosion) in the forward scan of the CP curve in Fig. 5.

Table 1 R_p values for the measurement after 72 h of exposure for different aluminum alloys from series 2xxx

Alloy	Average R_p [Ω]
AA2014	3348
AA2011	2865
AA2030	2571
EN AW 2030	1792
AA2024	1653

Fig. 5 CP measurements in the 5% NaCl solution for aluminum alloys from series 2xxx used in this study labeled E_{oc} and E_{rp}



Measurements of the Cyclic Polarization Curves

Figure 5 shows the values of the **corrosion potential** (E_{oc}) and the potential of the **repassivation or protective potential** (E_{rp}). The CP measurements show that none of the alloys had a typical breakdown potential, suggesting a shape of the CP curves that is typical for active corrosion. According to the potential of the scan reversal (the potential at which the current reaches 1 mA), the current in the cathodic direction is higher than that in the anodic direction. The latter shows that the aluminum alloys from series 2xxx used in this study can no longer be repassivated when the active corrosion begins [1]. The higher the $E_{oc}-E_{rp}$ potential difference, the better the materials' ability to repassivate. The $E_{oc}-E_{rp}$ trend of the potential difference is AA2024 > AA2030 > AA2014 > EN AW 2030 > AA2011 (see Table 2). This trend is given for information only, because these materials are not able to repassivate on their own in a 5% NaCl solution.

Electrochemical Fatigue

The analysis of the results of the fatigue measurements for the different aluminum alloys from series 2xxx is shown in Fig. 6. This analysis showed correlations between the

Table 2 E_{oc} , E_{rp} , and $E_{oc}-E_{rp}$ values for the applied aluminum alloys from series 2xxx

Alloy	E_{oc} [V]	E_{rp} [V]	$E_{oc}-E_{rp}$ [V]
AA2014	-0.653	-0.803	0.150
AA2011	-0.656	-0.771	0.115
AA2030	-0.587	-0.745	0.158
EN AW 2030	-0.598	-0.746	0.148
AA2024	-0.591	-0.784	0.193

fatigue time and the depth of the etching into the base material. Only the alloy AA2024 shows a significant deviation from the linearity of the depth of the etching into the base material from the time of the electrochemical fatigue. The equations of the calibration curves are given in Table 3.

Table 3 Equations of the lines for the dependence of the depth of etching in the base material (y) on the fatigue time (x)

Alloy	Equation of the line
AA2030	$y = 0.0281x - 12.25$
AA2014	$y = 0.0147x + 53.93$
AA2011	$y = 0.0137x + 23.86$
EN AW 2030	$y = 0.0023x + 5.16$

Fig. 6 Dependence of the etching depth on the electrochemical fatigue time

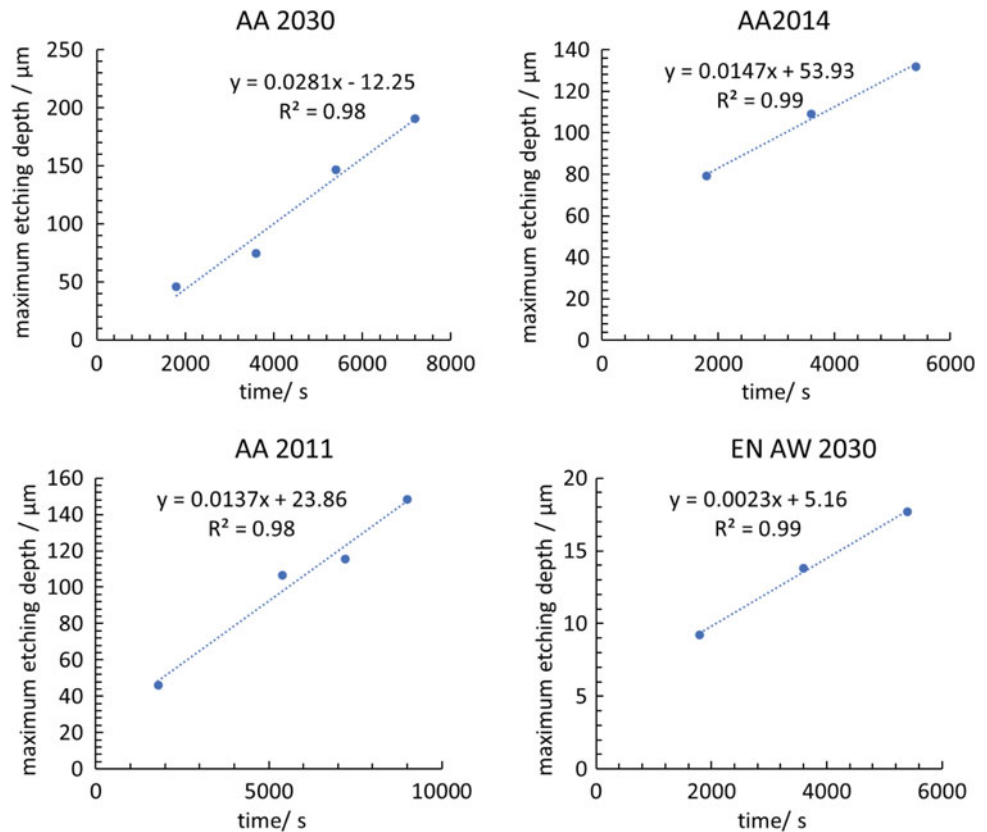


Table 4 Comparison of the maximum etching depths in the base material after the electrochemical fatigue and after the PV113 test

Alloy	Maximum etching depth (IGC) according to EC test [μm]	Maximum etching depth (IGC) according to PV113 test [μm]
AA2024	401	380
AA2011	306	242
AA2030	143	182
AA2014	260	150
EN AW 2030	147	150

Comparison of the Electrochemical Fatigue with the Standard PV113 Test

Table 4 shows the maximum etching depths of the base material (IGC) after the electrochemical fatigue tests and the PV113 test. The comparison clearly shows that intergranular corrosion occurred in a similar manner for the electrochemical fatigue and after the PV113 test (a similar trend is observed for the alloys). All the corrosion-depth measurements for the base material are very dependent on the measurement site, but the correlation was good nonetheless. It should be noted that the electrochemical fatigue test was performed in a 5% NaCl solution, while the PV113 test was performed in an HCl and H₂O₂ solution. Measurements in

the NaCl solution are certainly more representative of the corrosion of aluminum alloys, as these materials are not exposed to acids under oxidizing conditions. The corrosion is very dependent on the medium used (e.g., alloys in the automotive industry will be exposed primarily to chloride due to road gritting or salt from the sea, rather than acid and peroxide) [2–6].

Conclusions

We conducted an electrochemical corrosion study of five different aluminum alloys from series 2xxx (AA2024, AA2030, AA2014, EN AW 2030, and AA2011) in a 5%

NaCl solution, which is a highly corrosive medium for aluminum alloys. From this study, we can conclude:

- The alloy with the highest resistance to general corrosion is AA2014.
- A linear correlation between the depth of etching in the base material and the electrochemical fatigue time exists for the alloys AA2030, AA2014, EN AW 2030, and AA2011, whereas for alloy AA2024, this cannot be confirmed (additional measurements need to be made).
- There is a correlation between the electrochemical fatigue methods and the PV113 test for materials that are the most susceptible to intergranular corrosion.
- Electrochemical fatigue is suitable for inducing intergranular corrosion.

References

1. Khanari K, Finšgar M (2019) The Corrosion Inhibition of AA6082 Aluminium Alloy by Certain Azoles in Chloride Solution: Electrochemistry and Surface Analysis. *Coatings* 9(6):380
2. Khanari K, Finšgar M, Knez Hmcic M, Maver U, Knez Z, Seiti B (2017) Green corrosion inhibitors for aluminum and its alloys: a review. *RSC. Adv.* 7(44): 27299-2733
3. Wang J (2006) *Analytical Electrochemistry*. John Wiley & Sons, Inc., New Jersey
4. Finšgar M (2020) Surface analysis of the 2-mercaptobenzothiazole corrosion inhibitor on 6082 aluminum alloy using ToF-SIMS and XPS, *Analytical Methods* 12(4): 456–465
5. Khanari K, Finšgar M (2016) Organic corrosion inhibitors for aluminum and its alloys in acid solutions: a review, *Rsc Adv* 6(67): 62833–62857
6. Khanari K, Finšgar M (2019) Organic corrosion inhibitors for aluminum and its alloys in chloride and alkaline solutions: A review, *Arabian Journal of Chemistry* 12(8): 4646–4663